The CRISPR Journal
Volume 5, Number 2, 2022
Mary Ann Liebert, Inc.
DOI: 10.1089/crispr.2021.0129

The CRISPR Journal

Toward a CRISPR-Cas9-based Gene Drive in the Diamondback Moth *Plutella xylostella*

Xuejiao Xu,[1,2,†] Tim Harvey-Samuel,[3,†] Hamid Anees Siddiqui,[4] Joshua Xin De Ang,[3,i] Michelle Ellis Anderson,[3] Christine M. Reitmayer,[3] Erica Lovett,[3] Philip T. Leftwich,[5] Minsheng You,[1,*] and Luke Alphey[1,3,*]

Abstract

Promising to provide powerful genetic control tools, gene drives have been constructed in multiple dipteran insects, yeast, and mice for the purposes of population elimination or modification. However, it remains unclear whether these techniques can be applied to lepidopterans. Here, we used endogenous regulatory elements to drive Cas9 and single guide RNA (sgRNA) expression in the diamondback moth (DBM), *Plutella xylostella*, and test the first split gene drive system in a lepidopteran. The DBM is an economically important global agriculture pest of cruciferous crops and has developed severe resistance to various insecticides, making it a prime candidate for such novel control strategy development. A very high level of somatic editing was observed in Cas9/sgRNA transheterozygotes, although no significant homing was revealed in the subsequent generation. Although heritable Cas9-medated germline cleavage as well as maternal and paternal Cas9 deposition were observed, rates were far lower than for somatic cleavage events, indicating robust somatic but limited germline activity of Cas9/sgRNA under the control of selected regulatory elements. Our results provide valuable experience, paving the way for future construction of gene drives or other Cas9-based genetic control strategies in DBM and other lepidopterans.

Introduction

Gene drives are heritable elements capable of autonomously increasing their frequency within a gene pool.[1,2] Traits associated with the gene drive will also spread and could be arranged to include examples beneficial for pest control (e.g., a sex-specific fitness cost), reducing vector-borne virus transmission (e.g., virus-refractory transgenes), or conservation (e.g., resistance to disease/pesticides).[3,4]

One example of a gene drive technology is the CRISPR-Cas9-based homing drive.[4,5] In its simplest form, this system requires a source of Cas9 and a single guide RNA (sgRNA) expression cassette to be integrated into a genome at the precise site specified by the sgRNA. As this integrated ''homing element'' has disrupted its linked sgRNA site, it is immune to further cutting. However, in a heterozygote, the homologous ''wild-type'' (WT) chromosome may be targeted for cleavage by Cas9, and in the resulting double-strand break (DSB) repair, the locus harboring the integrated homing element may be used as a template for homology-directed repair (HDR), transforming the heterozygous cell into one homozygous for the homing element (a process known as ''homing''). If this process occurs in the germline, it can bias the inheritance of the homing element above the expected 50:50 ratio.[5]

The binary nature of the CRISPR-Cas9 system allows variations on this form, for example with one or both components integrated at sites away from the homing element. Such ''split-drive'' (sgRNA cassette remains in homing element)[6–9] or ''trans-drive'' (neither component remains in homing element)[10] designs are predicted to act in a more ''controllable'' way once released into a target population because any component not included in the homing

[1]*State Key Laboratory of Ecological Pest Control for Fujian and Taiwan Crops, Institute of Applied Ecology, Fujian Agriculture and Forestry University, Fuzhou, P.R. China;* [2]*School of Life Sciences, Peking University, Beijing, P.R. China;* [3]*Arthropod Genetics Group, The Pirbright Institute, Woking, Pirbright, United Kingdom;* [4]*National Institute for Biotechnology and Genetic Engineering, Faisalabad, Pakistan; and* [5]*School of Biological Sciences, University of East Anglia, Norwich, United Kingdom.*
[†]*These authors contributed equally to this work.*
[i]ORCID ID (https://orcid.org/0000-0002-4710-8831).

**Address correspondence to: Minsheng You, PhD, State Key Laboratory of Ecological Pest Control for Fujian and Taiwan Crops, Institute of Applied Ecology, Fujian Agriculture and Forestry University, Fuzhou, 350002, P.R. China,* Email: msyou@fafu.edu.cn *and Luke Alphey, PhD, Arthropod Genetics Group, The Pirbright Institute, Woking, Pirbright, GU24 0NF, United Kingdom*, Email: luke.alphey@pirbright.ac.uk

element will not benefit from super-Mendelian inheritance and will likely reduce in frequency over time due to associated fitness costs.[11,12] As both components are required in an individual for the drive to function, the efficiency of the drive will thus reduce over time as one or more components become limiting. Although potentially less efficient than the simple ''all in one'' design outlined above, the potential to limit the spread of a gene drive geographically and temporally may prove beneficial to the regulation, perception, and field deployment of such technologies.[13]

To date, CRISPR-Cas9 homing drives have been demonstrated in various dipterans (prominent examples include *Drosophila melanogaster*[14] and the mosquitoes *Anopheles gambiae*,[15] *Anopheles stephensi*,[16] and *Aedes aegypti*[17]), yeast,[6] and mice.[18] Here, we explore the potential of such technology for the first time in a lepidopteran—the diamondback moth (DBM) *Plutella xylostella*—focusing on a ''split-drive'' design. Lack of previous research into a lepidopteran gene drive is surprising, given the extreme and wide-ranging importance of this insect order, for example as major agricultural pests and invasive species,[19] and as producers of silk and components of industrial processes.[20] DBM provides an appropriate model for such work because it is both a globally important pest of brassica crops[21,22] and is tractable in terms of genetic engineering technologies, having been the subject of previous genetics-based pest control strategy development.[23,24]

Methods

Insects

DBM transgenic lines were generated from the Vero Beach WT strain,[25] with rearing conditions described previously.[26,27]

Identification and expression profiling of germline candidate genes

To drive Cas9 expression in specific tissues and developmental stages, germline-active promoters must be identified and characterized. Referring to previous reports,[28–31] amino acid sequences of nine germline candidates—*BGCN*, *Shutdown*, *SDS3*, *Meiw68*, *SIWI*, *NanosO*, *NanosP*, *NanosO*, and *NanosM* (origins listed in Supplementary Table S2)—were downloaded from the National Center for Biotechnology Information (https://www.ncbi.nlm.nih.gov/) and blasted against the DBM pacbiov1 genome database (http://ensembl.lepbase.org/Plutella_xylostella_pacbiov1/Info/Index) to identify putative homologs.

Expression patterns of these DBM candidates were compared with reverse transcription polymerase chain reaction (RT-PCR) using the endogenous gene *17S* as a loading control. DBM samples collected at different developmental stages (i.e., embryonic, larval, and adult stages) were dissected, frozen in liquid nitrogen, placed in RNAlater (Thermo Fisher Scientific), and stored at −80°C. Total RNA was extracted with the RNeasy Mini Kit (Qiagen), followed by removal of gDNA with DNase I (Thermo Fisher Scientific). Purified RNA was diluted to 20 ng/μL and used to produce cDNA pools with the RevertAid First Strand cDNA Synthesis Kit (Thermo Fisher Scientific). RT-PCR was conducted using the Q5 High-Fidelity 2×Master Mix (NEB). All primers used in the current study are available in Supplementary Table S1.

Construct design

Adult ovary total RNA was used to amplify the 5′ and 3′ UTR of *Pxmeiw68* and *PxnanosP* using the SMARTer RACE 5′/3′ Kit (Takara). Regulatory sequences 5′ and 3′ were then cloned from fourth instar larval gDNA (NucleoSpin Tissue Column; Macherey-Nagel). *PiggyBac* constructs AGG1906 (*Pxmeiw68-Cas9*; GenBank accession number OK145566) and AGG2093 (*PxnanosP-Cas9*; GenBank accession number OK145567) were developed as for AGG1536 (*Pxvasa-Cas9*) previously,[26] except for replacing the *Pxvasa* promoter, *Pxvasa* 3′ UTR, and SV40 terminator with corresponding regulatory fragments from *Pxmeiw68* and *PxnanosP* as well as the fluorophore marker 3′ UTR with P10. All plasmids were assembled with NEBuilder HiFi DNA Assembly Cloning Kit (NEB; see Fig. 1A).

For constructing sgRNA expressing lines (''homing elements''), two pigmentation genes *Pxyellow* and *Pxkmo*[27] were selected as targets for CRISPR-based site-specific insertion (''knock-in'') of sgRNA cassettes due to the ease of visually scoring null mutations in these genes. Between 800 and 1,000 bp upstream/downstream regions immediately flanking each sgRNA cleavage site were cloned from gDNA as homology arms for mediating HDR repair. Six RNA polymerase III *PxU6* promoters[32] were divided into two sets of three and used to express relevant sgRNAs for each gene (see Fig. 1B). Within each construct, although multiple U6 promoters were used, only a single sgRNA was expressed (all U6 promoters within the same construct expressed the same sgRNA). sgRNAs were designed with CHOPCHOP (https://chopchop.cbu.uib.no/). sgRNA expression cassettes were synthesized and cloned into the homology arm destination plasmid, alongside a Zsgreen-expressing marker (Fig. 1B; Genewiz; GenBank accession numbers AGG1619: OK145568, AGG1962:OK145570, and AGG1963: OK145569).

Assembled constructs were purified with NucleoBond Xtra Midi Prep Kit EF (Macherey-Nagel) before injection.

Development of transgenic lines

A *Pxvasa-Cas9* line (1536A) was built previously.[26] To mitigate issues associated with ''positional effects'' of the transgene insertion site, additional *Pxvasa-Cas9* lines were generated here, initially using the same method as previously described. Subsequently, to improve transformation efficiency, *piggyBac* helper plasmid and codon-optimized mRNA were replaced with a commercially synthesized *piggyBac* mRNA (TriLink Biotechnologies). Constructs (AGG1906 or AGG2093) were injected at 500 ng/μL alongside 600 ng/μL *piggyBac* mRNA to generate *Pxvasa-Cas9*, *Pxmeiw68-Cas9*, and *PxnanosP-Cas9* lines.

For constructing homing elements, sgRNAs were *in vitro* transcribed (150 ng/μL), complexed with 300 ng/μL Cas9 protein[27] and injected alongside the relevant sgRNA plasmid (800 ng/μL). Injection, transformant, and insertion-site identification were as previously described.[25,27]

For resolving the 5′ junction between the integrated homology arm and the genomic flanking sequence in 1619P15, the Cas9 Sequencing Kit (Oxford Nanopore Technologies) was used because PCR could not confirm the junction. In brief, high molecular weight (HMW) genomic gDNA was extracted from homozygous 1619P15 pupae using the Monarch HMW DNA extraction kit for tissue (NEB). The Cas9 Sequencing Kit (Oxford Nanopore Technology) was used to prepare a library targeting the insertion. Targets GAACTCGGT GATGACGTTCTCGG and GCTGAAGGGCGAGAC CCACAAGG were designed to target the DsRed open reading frame using CHOPCHOP and synthesized as Alt-R CRISPR-Cas9 crRNAs (IDT). These along with the Alt-R CRISPR-Cas9 tracrRNA and Alt-R SpCas9 Nuclease V3 (IDT) were used to digest the HMW gDNA following the manufacturer's instructions. Library was run on a MinION for 72 h with default parameters. Epi2me was used to map the resulting FASTQ files to the AGG1619 plasmid sequence as a reference, with 308 reads aligning. Further analysis was performed using Galaxy.[33] Porechop (v0.2.4; https://github.com/rrwick/Porechop) was used to trim adapters from all FASTQ files. All files were compiled into a single FASTA and filtered based upon alignment to the 5′ end of the homology arm in the reference sequence using Biopython.[34] The 46 remaining reads were manually mapped to the construct/genome interface.

The *Pxkmo* knockout line was generated previously.[27] The *Pxyellow* knockout line was generated following previous protocols,[35] except using a newly designed sgRNA (*Pxyellow-sgRNA4*) targeting the third *Pxyellow* exon.

Assessment of Cas9 somatic editing and homing efficiency

To assess somatic editing efficiency, reciprocal crosses were conducted using Cas9 and sgRNA lines. In each cross replicate, four Cas9 heterozygote ''grandparents'' and four sgRNA heterozygote ''grandparents'' were crossed, with F_1 eggs collected and reared until pupation. F_1 pupae were screened for fluorescence and body/eye pigmentation patterns based on mutant phenotypes reported previously.[27,35]

Note that *Pxyellow* mosaics are only observable when they co-occur in an individual displaying the ''stripy'' phenotype. This phenotype occurs naturally and consists of two darkly pigmented areas running laterally along the dorsal surface of the pupae. Therefore, the number of *Pxyellow* mosaics was calculated against the number displaying this phenotype rather than the total number of pupae. The mutagenesis of target sites was confirmed in a subset of somatic mosaics using a T7 endonuclease assay (NEB).

To assess ''homing'' activity, transheterozygous F_1s containing both Cas9 and sgRNA transgenes (parents) were selected from the above cross and themselves crossed to *Pxyellow* or *Pxkmo* knockout lines, depending on which sgRNA line was used in the initial cross (Fig. 3). In each cross replicate, a minimum of three transheterozygotes and three knockout individuals were reciprocally crossed, with five replicates conducted for each combination. An exception to the above process was made for the 1906 lines where, due to the large number of lines to assess, the ''grandparent'' factor was not applied.

In all cases, the third instar larvae (*Pxyellow* cross) or pupae (*Pxkmo* cross) of F_2 progeny were screened for fluorescence (to assess gene drive activity) and knockout phenotypes (to assess germline/somatic editing efficiency). Control crosses were conducted by reciprocally crossing each sgRNA line as heterozygotes to its respective knockout line and scoring the same details as above.

Statistical analyses

Analyses of sgRNA cassette inheritance was conducted using R v3.6.2 (The R Foundation for Statistical Computing),[36] and figures were generated using ggplot2[37] and patchwork.[38] The proportion of offspring inheriting the sgRNA cassette was analyzed using a binomial GLM (''logit'' link) with control cross outcomes set as the intercept. Approximate 95% confidence intervals were calculated using the Sidak adjustment for multiple comparisons.

Figures of germline cleavage percentages were made using GraphPad software. Differences were analyzed with one-way analysis of variance or an independent *t*-test using SPSS Statistics 22.0 (IBM Corp).

Western blot

Moth carcass, ovary, and testis samples from 2- to 3-day-old adults were homogenized on ice in 100 μL 1 × passive lysis buffer (PLB) including Halt Protease Inhibitor Cocktail (Thermo Fisher Scientific). After 15 min of incubation at room temperature, samples were centrifuged for 10 min at 10,000 *g* and 4°C. An additional 50 μL PLB + protease inhibitor was added to the samples and incubated for a further 15 min at room temperature.

Protein concentrations were determined using the DC Protein Assay (Bio-Rad) using a bovine serum albumin standard curve. Absorbance values were obtained using a microplate reader (GloMax) at 750 nm.

For each sample, equal amounts of total protein (35 μg) were combined with Laemmli sample buffer (Bio-Rad) and denatured for 5 min at 95°C.

Samples were loaded onto 4–20% precast polyacrylamide gels (Bio-Rad) and run at 200 V. A chemiluminescent protein ladder (8–260 kDa; LI-COR) was loaded alongside the protein samples to estimate the position of the 158 kDa Cas9 (FLAG-tagged) band. Proteins were transferred onto a nitrocellulose membrane (Bio-Rad). After transfer, unspecific binding sites were blocked overnight at 4°C with 3% milk powder (Marvel) in Tris-buffered saline solution (Bio-Rad) including 1% Tween 20 (TBS-Tween; Sigma–Aldrich). Anti-FLAG-tag antibody (Abcam) was diluted 1:1,000 in 3% milk/TBS-Tween, and the membrane incubated overnight at 4°C. Membranes were developed using Pierce ECL Western Blotting Substrate (Thermo Fisher Scientific), scanned using a Gel Doc imager (Bio-Rad), and analyzed using Image Lab software (Bio-Rad).

Results

Cas9 line generation and characterization

Previously, we showed that *Pxvasa* was preferentially expressed in adult soma and gonads, and the selected *Pxvasa* promoter fragment drove Cas9 somatic and gonadal transcription in a single generated line (1536A).[26] Here, three additional 1536 lines were developed (Fig. 1 and Table 1). Moreover, homologs of nine putative germline expressing genes were identified in DBM (Supplementary Table S2). RT-PCR showed that *Pxbgcn*, *Pxsds3*, *Pxshu1*, *Pxshu2*, *Pxpiwi*, and *PxnanosN* were ubiquitously transcribed in embryos, larvae, and adult tissues, whereas *PxnanosO* and *PxnanosM* were expressed in female ovaries and early embryos. In contrast, detectable *Pxmeiw68* expression was restricted to adult gonads, and *PxnanosP* was preferentially detected in adults (especially female ovaries; Supplementary Fig. S1A), making them better candidates for further construction of Cas9 lines for homing drive generation. The putative promoters and 5′/3′ regulatory regions of these two genes were cloned to direct Cas9 expression, with seven 1906 (*Pxmeiw68-Cas9*) and five 2093 (*PxnanosP-Cas9*) lines subsequently generated (Table 1). Flanking PCR confirmed independent insertion sites of each line (Supplementary Table S3). Paired expression profiling of Cas9 and endogenous genes (*Pxmeiw68*, *Pxvasa*, and *PxnanosP*) showed that Cas9 mRNA was transcribed in both testes and ovaries of all 1536, 2093, and 1906 lines except 1906B (Supplementary Fig. S1B). Unexpectedly, it was also observed that expression levels of Cas9 were much higher in adult carcasses than in gonads—the opposite trend for the respective endogenous genes (Supplementary Fig. S1B).

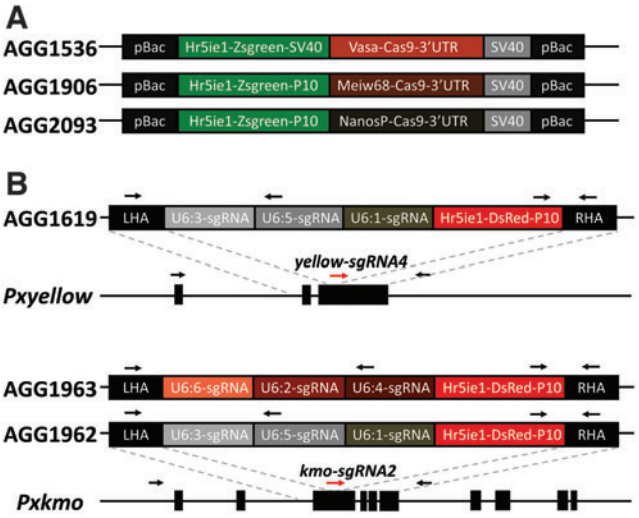

FIG. 1. Construction of transgenic lines. **(A)** Donor cassettes for *piggyBac*-mediated transformation of Cas9 lines. **(B)** Homology-directed repair (HDR)-based integration of homing elements into endogenous marker genes *Pxyellow* and *Pxkmo*. Note that the same single-guide RNA (sgRNA) was expressed by three different U6 promoters in each sgRNA donor construct. *Red arrow:* position of sgRNA target; *black arrow:* genotyping primers. Color images are available online.

sgRNA line generation and characterization

Homozygous null mutations in *Pxyellow* or *Pxkmo* cause visible phenotypes in the body or eye pigmentation of DBM, respectively, making them scorable markers for genome editing events.[27,35] As such we chose these two genes as targets for building sgRNA expression lines. Although six *PxU6* promoters (*PxU6:1* to *PxU6:6*) have been identified and characterized in DBM somatic cells,[32] no information is available on their germ-cell activities. Therefore, we employed a conservative approach,

Table 1. *PiggyBac*-based Construction of the *Pxmeiw68-Cas9* and *PxnanosP-Cas9* Transgenic Lines

Lines	Injection components	Injected eggs	Survival rate	Positive lines	Minimal transformation efficiency
Pxvasa-Cas9 (1536)	AGG1536 + AGG1533 + PxpBac mRNA	1,915	22.0% (421/1,915)	3	0.7%
Pxmeiw68-Cas9 (1906)	AGG1906 + AGG1533 + PxpBac mRNA	3,310	21.7% (719/3,310)	1	0.1%
Pxmeiw68-Cas9 (1906)	AGG1906 + AGG1533 + Synthesized CopBac mRNA	1,956	31.0% (607/1,956)	6	1.0%
PxnanosP-Cas9 (2093)	AGG2093 + Synthesized CopBac mRNA	3,242	24.2% (786/3,242)	19 (only five lines were kept)	2.4%
Pxyellow-sgRNA (1619)	AGG1619 + Cas9 protein + *yellow*-sgRNA4	~2,000	— (N/A)	2	— (N/A)
Pxkmo-sgRNA (1962)	AGG1962 + Cas9 protein + *kmo*-sgRNA2	2,432	19.9% (484/2,432)	2	0.4%
Pxkmo-sgRNA (1963)	AGG1963 + Cas9 protein + *kmo*-sgRNA2	2,168	18.5% (401/2,168)	3	0.7%

utilizing all six in two separate arrays (*PxU6:3,5,1* and *PxU6:6,2,4*) to express sgRNAs in three knock-in constructs (Fig. 1B). In each construct, the three chosen promoters each expressed an identical sgRNA, which was the sgRNA used to target the construct to its genomic location.

Using CRISPR-mediated site-specific knock-in, two AGG1619 lines (*yellow-sgRNA4* expressed by *PxU6:3,5,1* promoters), two AGG1962 lines (*kmo-sgRNA2* expressed by *PxU6:3,5,1* promoters), and three AGG1963 (*kmo-sgRNA2* expressed by *PxU6:6,2,4* promoters) lines were isolated (Table 1). Interestingly, PCR analysis of the genomic location of these lines revealed a high number of noncanonical repair events (Supplementary Fig. S2). Of the seven insertions, two were deemed ''off target,'' judging by the inability to generate PCR flanking bands and the lack of expected knockout phenotype in these lines when inbred (1962B, 1963A); two were in the correct locus but showed truncations of the outer transgene/homology arm sequences or genomic flanking regions (1619T18, 1962A); and three were perfectly integrated but displayed no (1619P15), very mild (1963C), or severe (1963B) internal deletions within the transgene sequence.

Note that the 5′ junction of 1619P15 could not be resolved by PCR and required targeted sequencing of the region to identify the repair junction (Cas9 Sequencing Kit; Oxford Nanopore Technology; Supplementary Figures S2 and S3). As 1619P15, 1962A, and 1963C were the most intact, each possessing a different sgRNA expression cassette and at least one perfectly repaired flanking sequence (both junctions perfectly repaired in 1963C and 1619P15), they were maintained for further cross experiments.

Somatic activity of CRISPR-Cas9 system (F_1 analysis)

To test the CRISPR-Cas9 system's ability to function when engineered into DBM, we first crossed heterozygous Cas9 and sgRNA F_0s and analyzed the phenotypes and genotypes of their F_1 progeny with regards to the target locus (*Pxyellow* or *Pxkmo*, respectively). Regarding insertion sites, these crosses theoretically resulted in four equally represented genotypes: *Cas9*-only, $target^{sgRNA}$ only, *Cas9* + $target^{sgRNA}$ transheterozygotes, and nonfluorescent WT.

Pxyellow analysis.

Broadly, *Pxyellow* somatic mosaics were observed in *Cas9* + $yellow^{sgRNA}$ transheterozygotes in all crosses involving 1536 and 2093 lines, while only two out of seven 1906 lines (1906B and 1906E) showed observable mosaicism in F_1s (Fig. 2A). Choosing a subset of these lines for finer-scale analysis, we calculated the somatic editing rates of F_1 individuals using 1536C, 1906B, 1906E, and 2093A (Table 2). All (100%) of $\frac{1536C}{+}$; $\frac{1619P15}{+}$, $\frac{1906B}{+}$; $\frac{1619P15}{+}$, and $\frac{2093A}{+}$; $\frac{1619P15}{+}$ were mosaic, while lower levels (72.7–85.7%) observed in $\frac{1906E}{+}$; $\frac{1619P15}{+}$ transheterozygous pupae. No mosaicism was observed in F_1s other than transheterozygotes, with the exception of $yellow^{sgRNA}$-only individuals, which were the progeny of Cas9 expressing 2093A mothers (27.2% mosaics), implying deposition of Cas9 through the maternal germline into the developing embryo in that line.

Pxkmo analysis.

Regarding crosses involving the 1963C line, *Pxkmo* mosaicism broadly concurred with *Pxyellow* results above. At a finer scale, however, the observable mosaic phenotype was generally lower in 1536C (54.4–84.3%), 1906B (4.0–9.7%), and 1906E (0–1.8%) F_1 transheterozygotes, although 100% of 2093A transheterozygotes continued to show some form of eye mosaicism (Table 3). Mosaicism of other F_1 genotypes was again absent except in crosses involving the 2093A line where it was present only in kmo^{sgRNA} individuals. Interestingly, however, here it occurred both where Cas9 had been deposited by the male (14% F_1 mosaic) and female (20.4% F_1 mosaic) parents.

A random subset of mosaic transheterozygotes were collected for both 1963C (*Pxkmo*) and 1619P15 (*Pxyellow*) crosses and editing events confirmed with a T7E1 mutagenesis assay (Supplementary Fig. S4).

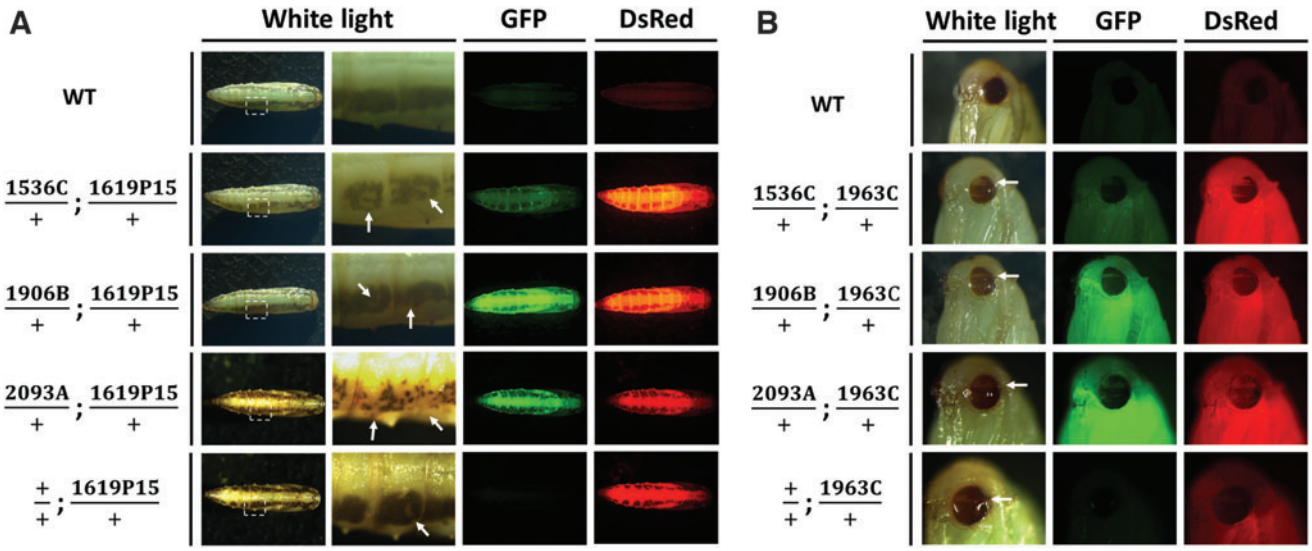

FIG. 2. Somatic mosaicism present in F_1 transheterozygotes. **(A)** Parental Cas9 lines were crossed with the 1619P15 line integrated into and expressing sgRNAs targeting *Pxyellow*. **(B)** Parental Cas9 lines are crossed with the 1963C line integrated into and expressing sgRNAs targeting *Pxkmo*. *White arrows:* mosaic phenotypes. Color images are available online.

Germline activity of CRISPR-Cas9 system (F_2 analysis)

F_1 transheterozygotes derived from the above experiments were reciprocally mated to relevant knockout lines (*Pxyellow*$^{-/-}$ for F_1s carrying 1619P15 and *Pxkmo*$^{-/-}$ for F_1s carrying 1963C/1962A), and their F_2 offspring were then scored for fluorescence and knockout phenotypes (Fig. 3). Under Mendelian inheritance, 50% of these F_2 would be expected to carry the relevant sgRNA-expressing transgene, with significant deviation above this taken to be an indication of inheritance bias caused by gene drive activity. For the control crosses, heterozygous Cas9 and sgRNA lines were independently, reciprocally, mated to the two knockout lines, with F_2 data collected as above (Supplementary Fig. S5).

Results showed no significant deviation from 50% inheritance for any of the three sgRNA-expressing transgenes assessed at a significance threshold of $p \leq 0.05$ (Fig. 4A), indicating that any gene drive activity, if present, was too low to detect. Interestingly, however, the observation of some WT and Cas9-only individuals with full *Pxkmo* or *Pxyellow* knockout phenotypes in the F_2 progeny indicated that germline expression and activity of Cas9 was nonetheless taking place (Fig. 4B), resulting in cleavage and repair through end joining rather than HDR/homing. These full knockout phenotypes could have derived from either cleavage of a parental WT chromosome in the F_1 germline or cutting in the F_2 following deposition of Cas9 by the F_1. Given that these individuals displayed full knockout phenotypes (complete white eyes or yellow bodies) rather than the mosaic phenotypes observed in the F1 analysis (where no such full knockout phenotypes were observed), we believe the former (germline

Table 2. Individuals and Percentages of Different Genotypes and Phenotypes Shown in F_1s Generated from *Pxyellow* Homing Crosses

	yellow^{sgRNA} *only*			*Cas9* + yellow^{sgRNA}			*Cas9 only*			*Nonfluorescence*		
Genotype Phenotype	*Total pupae*	*Stripy pupae*	*Mosaic stripy pupae*	*Total pupae*	*Stripy pupae*	*Mosaic stripy pupae*	*Total pupae*	*Stripy pupae*	*Mosaic stripy pupae*	*Total pupae*	*Stripy pupae*	*Mosaic stripy pupae*
1906B♂ × 1619P15♀	60	24	0	58	16	16 (100%)	80	30	0	73	27	0
1906B♀ × 1619P15♂	62	30	0	45	17	17 (100%)	61	30	0	68	27	0
1906E♂ × 1619P15♀	99	13	0	105	14	12 (85.7%)	77	7	0	100	27	0
1906E♀ × 1619P15♂	51	17	0	40	11	8 (72.7%)	28	7	0	45	14	0
1536C♂ × 1619P15♀	56	8	0	63	7	7 (100%)	58	18	0	52	16	0
1536C♀ × 1619P15♂	35	12	0	64	16	16 (100%)	46	19	0	57	16	0
2093A♂ × 1619P15♀	97	59	0	83	47	47 (100%)	72	40	0	86	45	0
2093A♀ × 1619P15♂	98	81	22 (27.2%)	92	84	84 (100%)	119	98	0	107	82	0

Table 3. Individuals and Percentages of Different Genotypes and Phenotypes Shown in F_1s Generated from *Pxkmo* Homing Crosses

Genotype	*Cas9 only*		*Cas9* + kmo^{sgRNA}		kmo^{sgRNA} *only*		*Non-fluorescence*	
Phenotype	*Total*	*Mosaic eye*	*Total*	*Mosaic eye*	*Total*	*Mosaic eye*	*Total*	*Mosaic eye*
1906B♂ × 1963♀	132	0	103	10 (9.7%)	122	0	135	0
1906B♀ × 1963♂	84	0	50	2 (4%)	69	0	75	0
1906E♂ × 1963♀	57	0	40	0 (0%)	41	0	66	0
1906E♀ × 1963♂	69	0	56	1 (1.8%)	71	0	68	0
1536C♂ × 1963♀	121	0	114	62 (54.4%)	105	0	129	0
1536C♀ × 1963♂	87	0	102	86 (84.3%)	82	0	81	0
2093A♂ × 1963♀	33	0	32	32 (100%)	43	6 (14%)	36	0
2093A♀ × 1963♂	39	0	32	32 (100%)	49	10 (20.4%)	42	0

cutting) hypothesis to be the more likely. It cannot be ruled out that very early cutting in the F_2 embryo may have contributed to this observation, however. Regarding 1619P15 (Fig. 4B-a), this activity was present in crosses involving the 1536 and 2093 but not 1906 lines.

Comparing putative germline cleavage rates by sex of transheterozygous F_1 parent between Cas9 lines, we found that 1536C and 2093A lines showed the highest average cleavage when assessing F_1 male parents (6.0% and 7.7%, respectively), whereas 1536C exhibited the highest average germline cutting when assessing F_1 female parents (2.9%). When comparing between sexes within each Cas9 line, the germline Cas9 activity in male transheterozygous parents was significantly higher than in female parents for both 1536C and 2093C crosses. Other comparisons were nonsignificant.

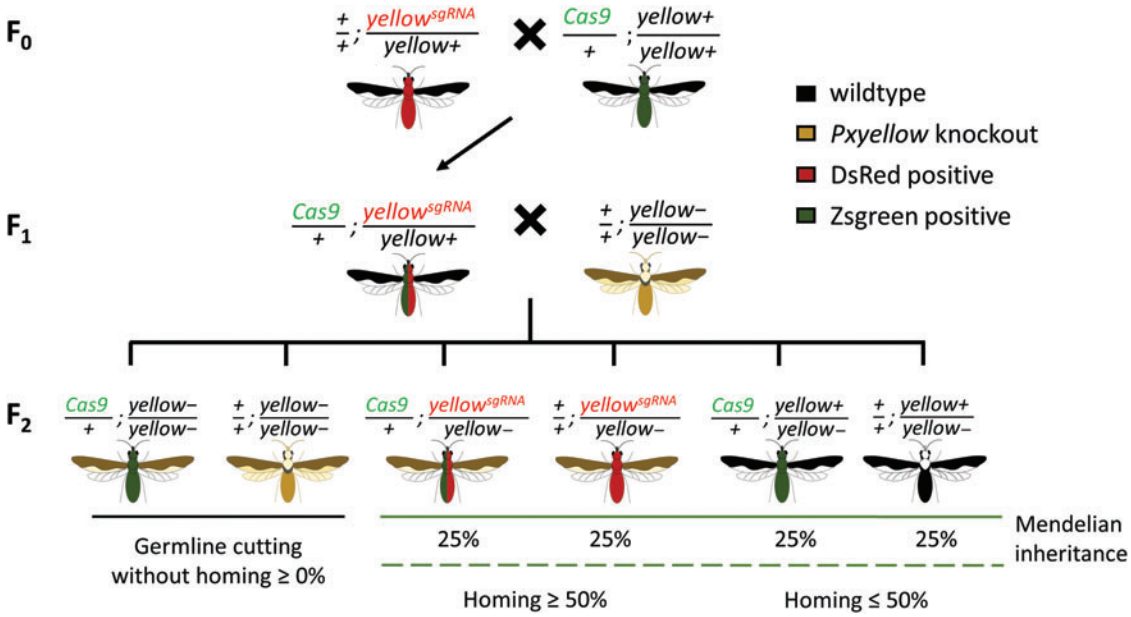

FIG. 3. Crossing scheme for the experiment. Taking the *Pxyellow* cross group for example, based on mendelian inheritance, only two pigmentation phenotypes as well as four genotypes will be observed in the F_2 generation: $\frac{yellowsgRNA}{yellow-}; \frac{Cas9}{+}$ (yellow pigmentation, DsRed positive, Zsgreen positive), $\frac{yellowsgRNA}{yellow-}; \frac{+}{+}$ (yellow pigmentation, DsRed positive, Zsgreen negative), $\frac{yellow+}{yellow-}; \frac{Cas9}{+}$ (wild-type [WT] pigmentation, DsRed negative, Zsgreen positive), $\frac{yellow+}{yellow-}; \frac{+}{+}$ (WT pigmentation, DsRed negative, Zsgreen negative), each representing 25% of the progeny, thus making the *yellow*^{sgRNA} (homing element) individuals = 50%. However, if germline cleavage and subsequent non-homologous end joining–based repair occurred, another two types—$\frac{yellow-}{yellow-}; \frac{Cas9}{+}$ (yellow pigmentation, DsRed negative, Zsgreen positive), $\frac{yellow-}{yellow-}; \frac{+}{+}$ (yellow pigmentation, DsRed negative, Zsgreen negative)—will occur. If homing were to occur in F_1 germlines, we would expect a bias in favor of individuals inheriting the *yellow*^{sgRNA} allele in the F_2 (>50%) at the expense of those not inheriting this element (<50%). As for targeting *Pxkmo*, in contrast to dark compound eyes in WT and heterozygous adults, homozygous null mutation of *Pxkmo* resulted in yellow eyes. Color images are available online.

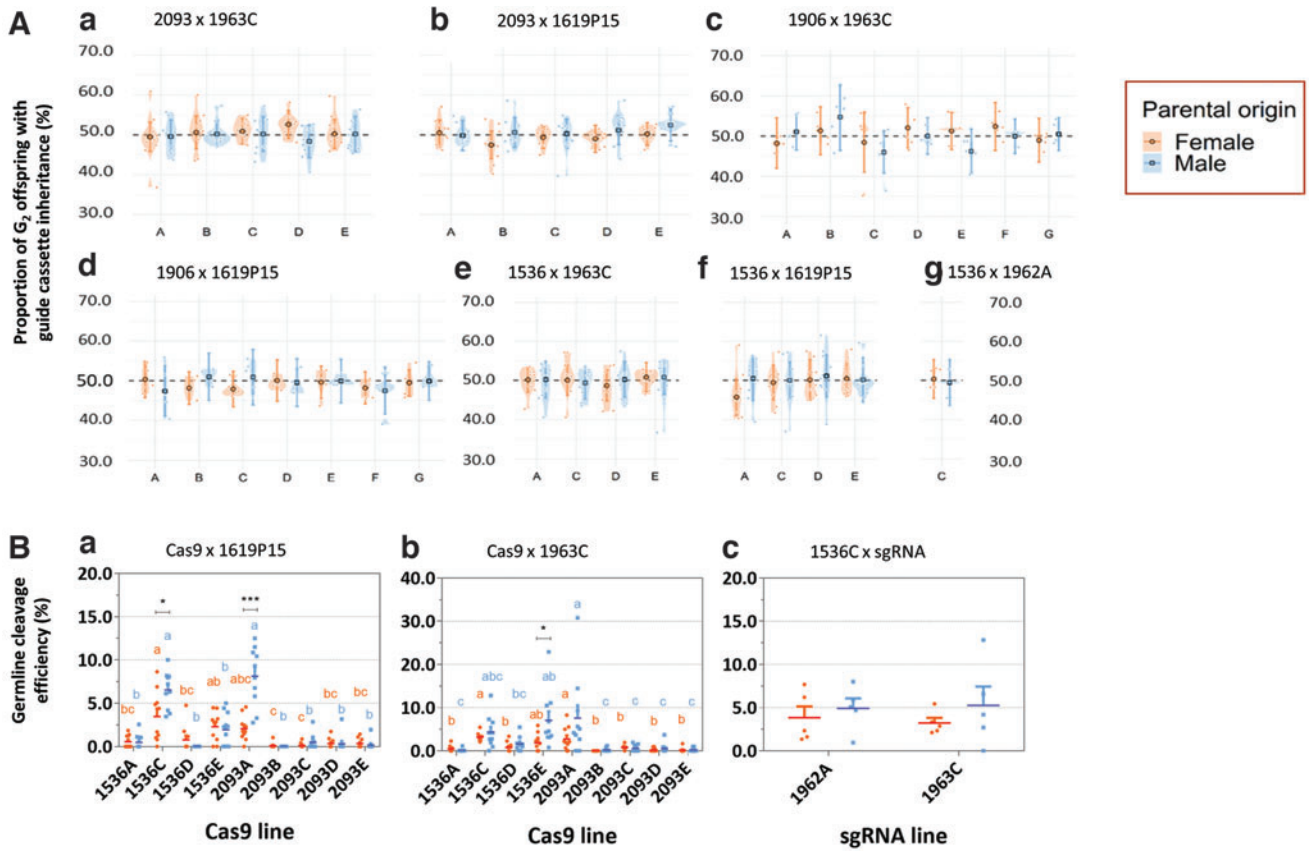

FIG. 4. Assessment of the inheritance of sgRNA cassettes and the germline cleavage efficiency. **(A)** Proportion of F_2 individuals inheriting the relevant homing element. Offspring come from either a male *(blue)* or female *(orange)* Cas9-bearing F_1 parent. Due to nonsignificant effect of "grandparental" (F_0) sex on the model, this factor has been collapsed in the data shown. Central tendency and error bars represent estimated mean proportions and associated approximate 95% confidence intervals for that treatment. Shaded areas (violin plots) represent the density distribution of the raw data. **(B)** Germline cleavage efficiency (%) = no. phenotypic mutants (e.g., yellow eyes)/[no. phenotypic mutants + phenotypic WT (e.g., black eyes)]. Offspring come from either a male *(blue)* or female *(orange)* Cas9-bearing F_1 parent. Data are plotted as means overlaid on raw data. For comparison of lines within the same sex, those that share a letter above the plotted data (e.g., ab and bc) are not significantly different from each other. For comparisons between sex, within each line: $*p < 0.05$; $**p < 0.01$; $***p < 0.001$. Color images are available online.

Similarly for crosses involving 1963C (Fig. 4B-b), putative germline cutting events were detected exclusively in F_1 WT and Cas9-only individuals from 1536 and 2093 crosses. Specifically, 2093A showed the highest germline editing levels, independent of whether assessing male or female F_1 transheterozygous parent (male F_1 = 7.6%, female F_1 = 2.8%). It was also noted that male F_1 parents showed higher germline cleavage rates than females in the 1536E crosses. To compare the cleavage efficiency induced by different *PxU6* promoters, we also conducted 1536C × 1962A crosses. Although null mutants derived from germline cleavage were also found in F_2s, no significant differences in frequency of these events were observed between 1962A and 1963C crosses involving 1536C (Fig. 4B-c).

A random selection of WT F_2 knockout mutants were individually sequenced at the relevant target site. Multiple indel alleles were observed separate from those previously established as occurring in each knockout line[27] (Supplementary Fig. S6).

Finally, gonads and carcasses of WT, 1536C, 2093A, and 2093D heterozygotes were dissected for comparing Cas9 protein expression. At a broad scale, it was noted that Cas9 protein levels generally appeared higher in

carcasses than gonads given equal amounts of total protein loaded (35 μg) in all three transgenic lines, while no Cas9 was expressed in WT (Supplementary Fig. S7)—a result in line with Cas9 transcription patterns detected by RT-PCR (Supplementary Fig. S1). However, unlike Cas9 mRNA patterns, Cas9 protein was not observed in 2093D gonads. This result concurs with the observation of both somatic and germline Cas9 activity (cutting) in the 1536C and 2093A lines but no germline activity in the 2093D line, strengthening the argument that cutting events detected in the F_2 generation resulted from Cas9/sgRNA activity in the F_1 germline.

Discussion

Previous studies integrating CRISPR-Cas9 components into lepidopterans are limited to the highly domesticated model species *Bombyx mori* (silkworm). There, using the IE1 promoter to drive Cas9 resulted in somatic editing of transheterozygotes[39–41] while using the *B. mori nanosP* promoter resulted in both somatic mosaicism of transheterozygotes[31,42–53] and some germline activity.[54–56] However, these studies provide no rates for these activities, and due to their experimental design, it is often difficult to disentangle the effects of germline edits from somatic mosaicism. Here, we expand the use of integrated CRISPR-Cas9 components to a free-living agricultural pest of global importance using an experimental design that allowed us to quantify and clarify different editing activities and also to assess the possibility of homing-based gene drive. Using three different endogenous promoters, which were putatively germline specific, we developed Cas9 expressing DBM lines. Testing these lines, we were able to demonstrate all three forms of Cas9 nuclease activity—*somatic expression*, resulting in mosaicism of F_1 transheterozygotes; *trans-generational deposition*, resulting in F_1 *target*^{sgRNA}-only mosaics; and *within germline expression*, resulting in F_2 nonfluorescent (WT) and Cas9-only target gene full-knockouts. Our results indicate that, in general, *Pxvasa-Cas9* and *PxnanosP-Cas9* drove higher rates of Cas9 activity than *Pxmeiw68-Cas9*.

We observed that somatic Cas9 expression from somatic activity of the *vasa* and *nanosP* promoters[14–16,57] was much enhanced relative to native *vasa* and *nanosP* in all Cas9 lines. This may be an interaction with the Hr5 enhancer used to aid expression of the fluorophore marker in our constructs. Although *nanosP* promoter activity has been reported as more germline restricted than *vasa* in *D. melanogaster*,[57,58] these two promoters both achieved high levels of somatic Cas9 expression in DBM, resulting in 100% observable mosaicism in multiple lines, similar to reports in *Drosophila suzukii* when the *vasa* and *nanos* promoters were used to drive Cas9.[63]

For some gene drive applications in DBM, it may be beneficial to reduce this somatic overexpression, for example by employing alternative regulatory elements without long-distance enhancers to drive marker expression, such as the 3xP3 or OpIE2 promoters, both of which have been characterized in lepidopteran transgenesis.[25] Nonetheless, ''leaky'' somatic expression of Cas9 may be a significant problem in constructing population-suppression gene drives targeting fertility/viability genes due to the generation of resistant alleles and the high fitness cost in drive heterozygotes.[59,60] On the other hand, the extremely high level of somatic editing activity demonstrated here would be of great utility in building alternative forms of genetic control technologies such as ''precision-guided SIT'' (pgSIT/TI-pgSIT),[61–63] HomeR drive,[64] and ClvR/TARE drive systems[65,66] by targeting essential fertility/viability genes. However, at least in the latter two technologies, this would need to be paired with significantly increased germline Cas9 activity. Future work could seek to identify suitable target genes for these phenotypes in DBM and utilize the novel tools generated here to arrange such a system for the first time in a lepidopteran.

Both maternal and paternal deposition of Cas9 occurred in *PxnanosP-Cas9*, although maternal Cas9 was more abundant, judging by mosaicism of *target*^{sgRNA}-only F_1 progeny. Our results contrast with a similar study in *D. melanogaster* where maternal but not paternal deposition of Cas9 was evident.[67] Similar deposition, however, was not observed in *Pxvasa-Cas9* lines, although such carryover occurs at high levels in *vasa-Cas9 A. gambiae*[59] and *vasa-Cas9 D. melanogaster*[67] transgenics, and Cas9 protein was clearly detected in the ovaries and testes of a *Pxvasa-Cas9* line here. It is possible that deposition of Cas9 protein or mRNA occurred in *Pxvasa-Cas9* lines but not at a level high enough to be observed in the relatively small areas (eyes and dorsal stripes) where mosaicism could be detected.

Germline activity of Cas9 was confirmed by the hypothesized inheritance of null *Pxkmo*/*Pxyellow* alleles by F_2 non-Cas9 (WT and *target*^{sgRNA}) individuals. However, compared with studies *in D. melanogaster*[60,67] where both *vasa* and *nanos* promoters have been tested, rates of germline cutting were relatively low, with a maximum mean of $8.1 \pm 1.0\%$ of WT chromosomes mutated. This was surprising because the high rate of somatic mosaicism observed suggested the expressed Cas9 protein and Pol III sgRNAs were highly capable of acting at the target site. A possible explanation could be either insufficient Cas9 expression/translation or sgRNA expression from the employed promoters within germline cells. While RT-PCR and Western blot analysis of gonads

from Cas9 lines confirmed the presence of Cas9 mRNA/protein, we cannot exclude the possibility that this may have largely represented expression within the somatic cells of gonadal tissues. Similar to studies assessing CRISPR-based split-drive in *A. aegypti*,[17] we observed that different Cas9 lines generated with a single construct (e.g., 2093A and 2093D) varied in Cas9 expression (RT-PCR and Western blot) and subsequent germline cleavage rates, likely due to the ''positional effect'' of semi-random *piggyBac* insertion. Future studies may seek to employ a site-specific approach once suitable ''safe-harbor'' sites have been identified, or an ''integral'' gene drive approach where endogenous regulatory elements can be hijacked for canonical Cas9 expression.[68] Interestingly, when comparing between sexes within each cross, significant differences (where they occurred) showed a higher level of cleavage in male rather than female germlines, whereas the opposite trend would have been expected given the endogenous expression patterns of *Pxvasa* and *PxnanosP*.

Germline editing and conversion rates can vary according to the locus being targeted by the homing element, likely affected by chromosome/chromatin structure, sgRNA efficiency, or sequence diversity in the population.[15,60] As such, we constructed sgRNA expressing lines by site specifically inserting guide cassettes into two loci: *Pxkmo* and *Pxyellow*. To our knowledge, this is the first report of HDR-based long fragment knock-in using CRISPR-Cas9 in the Lepidoptera, although site-specific integrations using the more complex microhomology-mediated end joining (MMEJ)-based PITCH technologies and TALEN-based integration have been demonstrated in *B. mori*.[44,69,70] However, knock-in efficiency was relatively low (0.4–0.7%), compared with highly efficient knockout in DBM (57.1%).[27] Integration rates were also lower than comparable reports in dipterans.[71–73] Interestingly, our results showed a large number of noncanonical repair events, with only two of the seven generated homing elements lines showing a precise, perfect integration. This runs contrary to experience in other insect species published,[17,57,70,73] and also our extensive experience in mosquitos, where off-target integration may occur relatively often, but those constructs integrated at the correct location are almost always integrated perfectly. A possible reason for imperfect integration detected here is that repeat sequences existing either inside the knock-in cassette (e.g., the multiple U6 promoters) or between the cassette and flanking genomic regions may have caused noncanonical repair of DSB (e.g., MMEJ) and the loss of partial knock-in sequences.[75] It is also noted that previous efforts to generate Cas9-mediated insertions using plasmid templates in *B. mori* have failed, while similar TALEN-based integrations are relatively efficient.[45] Therefore, it may be that some part of the DSB repair process in lepidopterans differs from other insects studied so far, reducing the efficiency of donor single-strand invasion following the blunt ends breaks created by Cas9, but not the overhanging breaks created by TALENs.

Other genome engineering tools (e.g., TALEN,[45,69] TAL-PITCH, and CRIS-PITCH[70]) could be employed to increase the integration efficiency of CRISPR-Cas9 split-drive components in DBM, although for this purpose the integration site mediated by these technologies would need to coincide fortuitously with the chosen sgRNA cleavage site. Additionally, we successfully utilized Cas9-based targeted sequencing of the integration junction to resolve the location of one of these homing element lines (1619P15). To our knowledge, this is the first published use of such a system and may be of benefit to other researchers seeking to resolve transgene integration junctions that are similarly difficult to resolve using conventional PCR-based techniques.

Despite testing three putatively germline-active Pol II promoters and six U6 Pol III promoters at two independent loci, we were unable to demonstrate significant gene drive. One explanation for this could include insufficient expression of Cas9 mRNA or its translation in tissues and at times required for a ''homing'' reaction to occur. The simultaneous presence of Cas9 protein and sgRNA in a germline-specific time window is critical for homing, especially in early meiosis when the germ cell is in a recombination-orientated state and homologous chromosomes are in close enough proximity to act as HDR templates.[67,76]

We were able to demonstrate here that Cas9 protein was present in gonadal tissues of both sexes and that it was able to mediate heritable germline DNA breakage events after complexing with sgRNAs. However, the timing of these events may have presented before or after this narrow window, and/or the expression levels might be too low in germ-cells to achieve distinguishable biases in inheritance, as has been similarly reported recently in mice.[77] As an additional hurdle, the imperfect repair of the 5′ homology arm/genome interface in 1962A may have reduced the ability of this integration to act as a repair template. This, however, did not apply to 1619P15 or 1963C, which were perfect integrations. Finally, we are unable to discount the possibility that the six known U6 promoters in DBM do not function efficiently in the germline. We recommend additional germline-specific regulatory components to be tested in DBM to increase germline cleavage and conversion efficiency.

Conclusion

In summary, this study has identified and characterized endogenous genetic components (i.e., germline active Pol II and Pol III promoters) and completed the first CRISPR-mediated site-specific knock-in of large fragments in the Lepidoptera. With these components, we built and tested the first split-drive system in a lepidopteran, achieving a very high level of somatic editing. Although we did not see significant homing, Cas9-mediated germline cleavage as well as maternal and paternal Cas9 deposition was observed. Our results provide valuable experience, paving the way for future construction of gene drives, or other Cas9-based genetic control strategies in the global pest, DBM, and other lepidopterans.

Acknowledgments

A previous version of this manuscript was published as a preprint on bioRxiv and is available at https://doi.org/10.1101/2021.10.05.462963.

Author Disclosure Statement

No competing financial interests exist.

Funding Information

This work was supported by European Union H2020 Grant nEUROSTRESSPEP (634361). In addition, THS and LA were respectively supported by a Impact Acceleration Account grant (BB/S506680/1), and three core fundings [BBS/E/I/00007033, BBS/E/I/00007038 and BBS/E/I/00007039] from the UK Biotechnology and Biological Sciences Research Council. XX was supported by a CSC Scholarship from the Chinese Government.

Supplementary Material

Supplementary Figure S1
Supplementary Figure S2
Supplementary Figure S3
Supplementary Figure S4
Supplementary Figure S5
Supplementary Figure S6
Supplementary Figure S7
Supplementary Table S1
Supplementary Table S2
Supplementary Table S3

References

1. Sinkins SP, Gould F. Gene drive systems for insect disease vectors. *Nat Rev Genet* 2006;7:427–435. DOI: 10.1038/nrg1870.
2. Champer J, Buchman A, Akbari OS. Cheating evolution: engineering gene drives to manipulate the fate of wild populations. *Nat Rev Genet* 2016;17:146–159. DOI: 10.1038/nrg.2015.34.
3. Alphey L. Genetic control of mosquitoes. *Annu Rev Entomol* 2014;59:205–224. DOI: 10.1146/annurev-ento-011613-162002.
4. Esvelt KM, Smidler AL, Catteruccia F, et al. Concerning RNA-guided gene drives for the alteration of wild populations. *eLife* 2014;3:e03401. DOI: 10.7554/eLife.03401.
5. Burt A. Site-specific selfish genes as tools for the control and genetic engineering of natural populations. *Proc Biol Sci* 2003;270:921–928. DOI: 10.1098/rspb.2002.2319.
6. DiCarlo JE, Chavez A, Dietz SL, et al. Safeguarding CRISPR-Cas9 gene drives in yeast. *Nat Biotechnol* 2015;33:1250–1255. DOI: 10.1038/nbt.3412.
7. Noble C, Min J, Olejarz J, et al. Daisy-chain gene drives for the alteration of local populations. *Proc Natl Acad Sci U S A* 2019;116:8275–8282. DOI: 10.1073/pnas.1716358116.
8. López Del Amo V, Bishop AL, Sánchez C HM, et al. A transcomplementing gene drive provides a flexible platform for laboratory investigation and potential field deployment. *Nat Commun* 2020;11:352. DOI: 10.1038/s41467-019-13977-7.
9. Gantz VM, Bier E. The dawn of active genetics. *BioEssays* 2016;38:50–63. DOI: 10.1002/bies.201500102.
10. Guichard A, Haque T, Bobik M, et al. Efficient allelic-drive in *Drosophila*. *Nat Commun* 2019;10:1640. DOI: 10.1038/s41467-019-09694-w.
11. Terradas G, Buchman AB, Bennett JB, et al. Inherently confinable split-drive systems in *Drosophila*. *Nat Commun* 2021;12:1480. DOI: 10.1038/s41467-021-21771-7.
12. Dhole S, Vella MR, Lloyd AL, et al. Invasion and migration of spatially self-limiting gene drives: a comparative analysis. *Evol Appl* 2018;11:794–808. DOI: 10.1111/eva.12583.
13. Harvey-Samuel T, Campbell K, Edgington M, et al. Trialling gene drives to control invasive species: what, where and how? In Veitch CR, Clout MN, Martin AR, et al. (eds). Island Invasives: Scaling Up to Meet the Challenge, Occasional Paper SSC no. 62. Gland, Switzerland: IUCN, 2019, 618–627.
14. Gantz VM, Bier E. Genome editing. The mutagenic chain reaction: a method for converting heterozygous to homozygous mutations. *Science* 2015;348:442–444. DOI: 10.1126/science.aaa5945.
15. Hammond A, Galizi R, Kyrou K, et al. A CRISPR-Cas9 gene drive system targeting female reproduction in the malaria mosquito vector *Anopheles gambiae*. *Nat Biotechnol* 2016;34:78–83. DOI: 10.1038/nbt.3439.
16. Gantz VM, Jasinskiene N, Tatarenkova O, et al. Highly efficient Cas9-mediated gene drive for population modification of the malaria vector mosquito *Anopheles stephensi*. *Proc Natl Acad Sci U S A* 2015;112:E6736–E6743. DOI: 10.1073/pnas.1521077112.
17. Li M, Yang T, Kandul NP, et al. Development of a confinable gene drive system in the human disease vector *Aedes aegypti*. *eLife* 2020;9:e51701. DOI: 10.7554/eLife.51701.
18. Grunwald HA, Gantz VM, Poplawski G, et al. Super-Mendelian inheritance mediated by CRISPR-Cas9 in the female mouse germline. *Nature* 2019;566:105–109. DOI: 10.1038/s41586-019-0875-2.
19. Suckling DM, Conlong DE, Carpenter JE, et al. Global range expansion of pest Lepidoptera requires socially acceptable solutions. *Biol Invasions* 2017;19:1107–1119. DOI: 10.1007/s10530-016-1325-9.
20. Ejiofor AO. Insect biotechnology. In Raman C, Goldsmith MR, Tolulope A, et al. (eds). Short Views on Insect Genomics and Proteomics: Insect Proteomics, Vol. 2. Cham, Switzerland: Springer, 2016, 185–210.
21. Furlong MJ, Wright DJ, Dosdall LM. Diamondback moth ecology and management: problems, progress, and prospects. *Annu Rev Entomol* 2013;58:517–541. DOI: 10.1146/annurev-ento-120811-153605.
22. Li Z, Feng X, Liu SS, et al. Biology, ecology, and management of the diamondback moth in China. *Annu Rev Entomol* 2016;61:277–296. DOI: 10.1146/annurev-ento-010715-023622.
23. Jin L, Walker AS, Fu G, et al. Engineered female-specific lethality for control of pest Lepidoptera. *ACS Synth Biol* 2013;2:160–166. DOI: 10.1021/sb300123m.
24. Harvey-Samuel TD, Xu X, Lovett E, et al. Engineered expression of the invertebrate-specific scorpion toxin AaHIT reduces adult longevity and female fecundity in the diamondback moth *Plutella xylostella*. *Pest Manag Sci* 2021;77:3154–3164. DOI: 10.1002/ps.6353.
25. Martins S, Naish N, Walker AS, et al. Germline transformation of the diamondback moth, *Plutella xylostella* L., using the *piggyBac* transposable element. *Insect Mol Biol* 2012;21:414–421. DOI: 10.1111/j.1365-2583.2012.01146.x.
26. Xu X, Yang J, Harvey-Samuel T, et al. Identification and characterization of the *vasa* gene in the diamondback moth, *Plutella xylostella*. *Insect Biochem Mol Biol* 2020;122:103371. DOI: 10.1016/j.ibmb.2020.103371.
27. Xu X, Harvey-Samuel T, Yang J, et al. Ommochrome pathway genes *kynurenine 3-hydroxylase* and *cardinal* participate in eye pigmentation

in *Plutella xylostella*. *BMC Mol Cell Biol* 2020;21:63. DOI: 10.1186/s12860-020-00308-8.
28. Kawaoka S, Minami K, Katsuma S, et al. Developmentally synchronized expression of two *Bombyx mori* Piwi subfamily genes, *SIWI* and *BmAGO3* in germ-line cells. *Biochem Biophys Res Commun* 2008;367:755–760. DOI: 10.1016/j.bbrc.2008.01.013.
29. Hagen DE. Identification and characterization of germline-specific promoters for remobilization of transgenes in the mosquitoes, *Aedes aegypti* and *Anopheles gambiae*. DPhil thesis, Texas A&M University, 2009.
30. Verkuijl SAN, Gonzalez E, Li M, et al. A CRISPR endonuclease gene drive reveals two distinct mechanisms of inheritance bias. *bioRxiv* 2020;2020.2012.2015.421271. DOI: 10.1101/2020.12.15.421271.
31. Xu J, Chen RM, Chen SQ, et al. Identification of a germline-expression promoter for genome editing in *Bombyx mori*. *Insect Sci* 2019;26:991–999. DOI: 10.1111/1744-7917.12657.
32. Huang Y, Wang Y, Zeng B, et al. Functional characterization of Pol III U6 promoters for gene knockdown and knockout in *Plutella xylostella*. *Insect Biochem Mol Biol* 2017;89:71–78. DOI: 10.1016/j.ibmb.2017.08.009.
33. Cock PJ, Grüning BA, Paszkiewicz K, et al. Galaxy tools and workflows for sequence analysis with applications in molecular plant pathology. *PeerJ* 2013;1:e167. DOI: 10.7717/peerj.167.
34. Cock PJA, Antao T, Chang JT, et al. Biopython: freely available Python tools for computational molecular biology and bioinformatics. *Bioinformatics* 2009;25:1422–1423. DOI: 10.1093/bioinformatics/btp163.
35. Wang Y, Huang Y, Xu X, et al. CRISPR/Cas9-based functional analysis of *yellow* gene in the diamondback moth, *Plutella xylostella*. *Insect Sci* 2021;28:1504–1509. DOI: 10.1111/1744-7917.12870.
36. R Core Team. R: A language and environment for statistical computing. R Foundation for Statistical Computing, Vienna, Austria 2018. Available online at: https://www.R-project.org/
37. Wickham H. ggplot2—Elegant Graphics for Data Analysis. Cham, Switzerland: Springer International Publishing, 2016.
38. Pedersen TL. Patchwork: The Composer of Plots. *R package version 1.0. 0*. 2019
39. Li Z, You L, Yan D, et al. *Bombyx mori* histone methyltransferase *BmAsh2* is essential for silkworm piRNA-mediated sex determination. *PloS Genet* 2018;14:e1007245. DOI: 10.1371/journal.pgen.1007245.
40. Li Z, You L, Zeng B, et al. Ectopic expression of ecdysone oxidase impairs tissue degeneration in *Bombyx mori*. *Proc Royal Soc B* 2015;282:20150513. DOI: 10.1098/rspb.2015.0513.
41. Zeng B, Zhan S, Wang Y, et al. Expansion of CRISPR targeting sites in *Bombyx mori*. *Insect Biochem Mol Biol* 2016;72:31–40. DOI: 10.1016/j.ibmb.2016.03.006.
42. Xu J, Yu Y, Chen K, et al. Intersex regulates female external genital and imaginal disc development in the silkworm. *Insect Biochem Mol Biol* 2019;108:1–8. DOI: 10.1016/j.ibmb.2019.02.003.
43. Xu X, Wang YH, Liu ZL, et al. Disruption of egg-specific protein causes female sterility in *Bombyx mori*. *Insect Sci* 2021 Feb 24 [Epub ahead of print]; DOI: 10.1111/1744-7917.12904.
44. Xu J, Chen S, Zeng B, et al. *Bombyx mori* P-element Somatic Inhibitor (BmPSI) is a key auxiliary factor for silkworm male sex determination. *PloS Genet* 2017;13:e1006576. DOI: 10.1371/journal.pgen.1006576.
45. Zhang Z, Niu B, Ji D, et al. Silkworm genetic sexing through W chromosome-linked, targeted gene integration. *Proc Natl Acad Sci U S A* 2018;115:8752–8756. DOI: 10.1073/pnas.1810945115.
46. Chen K, Yu Y, Yang D, et al. *Gtsf1* is essential for proper female sex determination and transposon silencing in the silkworm, *Bombyx mori*. *PloS Genet* 2020;16:e1009194. DOI: 10.1371/journal.pgen.1009194.
47. Chen K, Chen S, Xu J, et al. *Maelstrom* regulates spermatogenesis of the silkworm, *Bombyx mori*. *Insect Biochem Mol Biol* 2019;109:43–51. DOI: 10.1016/j.ibmb.2019.03.012.
48. Xu X, Wang Y, Bi H, et al. Mutation of the seminal protease gene, *serine protease 2*, results in male sterility in diverse lepidopterans. *Insect Biochem Mol Biol* 2020;116:103243. DOI: 10.1016/j.ibmb.2019.103243.
49. Xu X, Zhang Z, Yang Y, et al. Genome editing reveals the function of *Yorkie* during the embryonic and early larval development in silkworm, *Bombyx mori*. *Insect Mol Biol* 2018;27:675–685. DOI: 10.1111/imb.12502.
50. Chen S, Liu Y, Yang X, et al. Dysfunction of dimorphic sperm impairs male fertility in the silkworm. *Cell Discov* 2020;6:60. DOI: 10.1038/s41421-020-00194-6.
51. Zhang R, Zhang Z, Huang Y, et al. A single ortholog of *teashirt* and *tiptop* regulates larval pigmentation and adult appendage patterning in *Bombyx mori*. *Insect Biochem Mol Biol* 2020;121:103369. DOI: 10.1016/j.ibmb.2020.103369.
52. Bi H, Xu X, Li X, et al. CRISPR disruption of *BmOvo* resulted in the failure of emergence and affected the wing and gonad development in the silkworm *Bombyx mori*. *Insects* 2019;10:254. DOI: 10.3390/insects10080254.
53. Xu X, Bi H, Wang Y, et al. Disruption of the *ovarian serine protease* (*Osp*) gene causes female sterility in *Bombyx mori* and *Spodoptera litura*. *Pest Manag Sci* 2020;76:1245–1255. DOI: 10.1002/ps.5634.
54. Xu J, Liu W, Yang D, et al. Regulation of olfactory-based sex behaviors in the silkworm by genes in the sex-determination cascade. *PloS Genet* 2020;16:e1008622. DOI: 10.1371/journal.pgen.1008622.
55. Nartey MA, Sun X, Qin S, et al. CRISPR/Cas9-based knockout reveals that the clock gene *timeless* is indispensable for regulating circadian behavioral rhythms in *Bombyx mori*. *Insect Sci* 2021;28:1414–1425. DOI: 10.1111/1744-7917.12864.
56. Liu Q, Liu W, Zeng B, et al. Deletion of the *Bombyx mori* odorant receptor co-receptor (*BmOrco*) impairs olfactory sensitivity in silkworms. *Insect Biochem Mol Biol* 2017;86:58–67. DOI: 10.1016/j.ibmb.2017.05.007.
57. Gratz SJ, Ukken FP, Rubinstein CD, et al. Highly specific and efficient CRISPR/Cas9-catalyzed homology-directed repair in *Drosophila*. *Genetics* 2014;196:961–971. DOI: 10.1534/genetics.113.160713.
58. Port F, Chen HM, Lee T, et al. Optimized CRISPR/Cas tools for efficient germline and somatic genome engineering in *Drosophila*. *Proc Natl Acad Sci U S A* 2014;111:E2967–E2976. DOI: 10.1073/pnas.1405500111.
59. Hammond AM, Kyrou K, Bruttini M, et al. The creation and selection of mutations resistant to a gene drive over multiple generations in the malaria mosquito. *PloS Genet* 2017;13:e1007039. DOI: 10.1371/journal.pgen.1007039.
60. Champer J, Reeves R, Oh SY, et al. Novel CRISPR/Cas9 gene drive constructs reveal insights into mechanisms of resistance allele formation and drive efficiency in genetically diverse populations. *PloS Genet* 2017;13:e1006796. DOI: 10.1371/journal.pgen.1006796.
61. Li M, Yang T, Bui M, et al. Suppressing mosquito populations with precision guided sterile males. *Nat Commun* 2021;12:5374. DOI: 10.1038/s41467-021-25421-w.
62. Kandul NP, Liu J, Sanchez C HM, et al. Transforming insect population control with precision guided sterile males with demonstration in flies. *Nat Commun* 2019;10:84. DOI: 10.1038/s41467-018-07964-7.
63. Kandul NP, Liu J, Akbari OS. Temperature-inducible precision guided sterile insect Technique. *bioRxiv* 2021;2021.2006.2014.448312. DOI: 10.1101/2021.06.14.448312.
64. Kandul NP, Liu J, Bennett JB, et al. A confinable home-and-rescue gene drive for population modification. *eLife* 2021;10:e65939. DOI: 10.7554/eLife.65939.
65. Oberhofer G, Ivy T, Hay BA. Cleave and Rescue, a novel selfish genetic element and general strategy for gene drive. *Proc Natl Acad Sci U S A* 2019;116:6250–6259. DOI: 10.1073/pnas.1816928116.
66. Champer J, Lee E, Yang E, et al. A toxin-antidote CRISPR gene drive system for regional population modification. *Nat Commun* 2020;11:1082. DOI: 10.1038/s41467-020-14960-3.
67. Champer J, Liu J, Oh SY, et al. Reducing resistance allele formation in CRISPR gene drive. *Proc Natl Acad Sci U S A* 2018;115:5522–5527. DOI: 10.1073/pnas.1720354115.
68. Nash A, Urdaneta GM, Beaghton AK, et al. Integral gene drives for population replacement. *Biol Open* 2019;8:bio037762. DOI: 10.1242/bio.037762.
69. Wang Y, Tan A, Xu J, et al. Site-specific, TALENs-mediated transformation of *Bombyx mori*. *Insect Biochem Mol Biol* 2014;55:26–30. DOI: 10.1016/j.ibmb.2014.10.003.
70. Sakuma T, Nakade S, Sakane Y, et al. MMEJ-assisted gene knock-in using TALENs and CRISPR-Cas9 with the PITCh systems. *Nat Protoc* 2016;11:118–133. DOI: 10.1038/nprot.2015.140.
71. Purusothaman D-K, Shackleford L, Anderson M, et al. CRISPR/Cas-9 mediated knock-in by homology dependent repair in the West Nile Virus vector *Culex quinquefasciatus* Say. *Sci Rep* 2021;11:14964. DOI: 10.1038/s41598-021-94065-z.

72. Sun D, Guo Z, Liu Y, et al. Progress and prospects of CRISPR/Cas systems in insects and other arthropods. *Front Physiol* 2017;8:608–608. DOI: 10.3389/fphys.2017.00608.
73. Gratz SJ, Wildonger J, Harrison MM, et al. CRISPR/Cas9-mediated genome engineering and the promise of designer flies on demand. *Fly* 2013;7:249–255. DOI: 10.4161/fly.26566.
74. Gilles AF, Schinko JB, Averof M. Efficient CRISPR-mediated gene targeting and transgene replacement in the beetle *Tribolium castaneum*. *Development* 2015;142:2832–2839. DOI: 10.1242/dev.125054.
75. Verma P, Greenberg RA. Noncanonical views of homology-directed DNA repair. *Genes Dev* 2016;30:1138–1154. DOI: 10.1101/gad.280545.116.
76. Champer J, Chung J, Lee YL, et al. Molecular safeguarding of CRISPR gene drive experiments. *eLife* 2019;8. DOI: 10.7554/eLife.41439.
77. Pfitzner C, White MA, Piltz SG, et al. Progress toward zygotic and germline gene drives in mice. *CRISPR J* 2020;3:388–397. DOI: 10.1089/crispr.2020.0050.